



Lithium perchlorate modified nanoporous polyethersulfone membranes for improved dye rejection

K. Rambabu^{a,*}, S. Gokul^a, A.S. Russel^a, Akella Sivaramakrishna^b,
Babu Ponnusami^a, Fawzi Banat^c

^aDepartment of Chemical Engineering, School of Civil and Chemical Engineering, Vellore Institute of Technology, Vellore 632014, India, email: rambabu.k@vit.ac.in (K. Rambabu)

^bDepartment of Chemistry, School of Advanced Sciences, Vellore Institute of Technology, Vellore 632014, Tamil Nadu, India

^cDepartment of Chemical Engineering, Khalifa University of Science and Technology, The Petroleum Institute, Abu Dhabi, UAE

Received 27 March 2018; Accepted 27 June 2018

ABSTRACT

Nanoporous polyethersulfone (PES) membranes were synthesized using lithium perchlorate (LiClO_4) as an additive in the casting dope. Membranes were prepared through phase inversion method from PES/polyethylene glycol (PEG)/ LiClO_4 system using dimethylformamide (DMF) as the primary solvent and water as secondary solvent. Effect of LiClO_4 on the membrane performance was studied by varying its composition from 0 wt% to 5 wt%. SEM studies indicated that the LiClO_4 blended PES membranes possessed dense top surface and finger-like sub-layer. Atomic force microscopy analysis clearly showed that the addition of LiClO_4 resulted in nano-structure membranes with small surface pore size and low surface roughness. Contact angle measurements confirmed the enhanced hydrophilicity of the composite membranes due to LiClO_4 inclusion. Pure water flux measurements demonstrated high flux capabilities of LiClO_4 blended PES membranes as compared with pristine PES membrane. Dye rejection performance studies using Congo red, Crystal violet and Methylene blue as probe molecules, indicated a better dye removal efficiency of the LiClO_4 incorporated PES membrane. Fouling analysis in terms of fouling recovery ratio exhibited the better anti-fouling ability of the PES membranes due to LiClO_4 incorporation. Analysis on the obtained result showed that the 3 wt% LiClO_4 blended PES membrane possessed desirable characteristics among the synthesized PES/PEG/ LiClO_4 membrane series.

Keywords: Polyethersulfone; Lithium perchlorate; Nanoporous; Membrane; Dye rejection; Anti-fouling

1. Introduction

Increased demand for textile products has resulted in tremendous growth of textile industries in India, especially in the last two decades. These industries produce a large amount of dye polluted wastewater which has to be effectively treated for safe discharge of the effluent. Membrane separation is a more promising technology to handle this issue with several advantages as compared with

other conventional processes [1]. These advantages include low investment, compact nature, low energy consumption, room temperature operation and less pollution [2,3]. Polyethersulfone (PES) is one of the best starting materials for polymeric membrane preparation for water and wastewater treatment [4]. PES has many merits such as high chemical resistance, wide range of pH tolerance, desirable mechanical properties and ease of fabrication. PES has been used in preparation of asymmetric ultrafiltration and nanofiltration

* Corresponding author.

Presented at the 3rd International Conference on Recent Advancements in Chemical, Environmental and Energy Engineering, 15–16 February, Chennai, India, 2018.

membranes with different pore sizes and varying surface geometry [5,6]. However, PES based membranes often suffer from membrane fouling, when applied to water and wastewater treatment, due to its high hydrophobic nature [7]. Consequently, modification of PES membrane is a vital step to improve its hydrophilic ability and thereby the anti-fouling property of the membrane.

Inclusion of a hydrophilic additive to the casting solution of the membrane system is a simple and effective method of producing hydrophilic membranes with better anti-fouling ability [8,9]. It has been reported that inclusion of inorganic oxides/salts to PES membrane enhances the hydrophilicity of the resulting PES blend system [10–12]. These additives create a desirable membrane structure by preventing macrovoids establishment, enhancing pore formation, extending pore interconnectivity and introducing hydrophilicity [13]. The enhanced anti-fouling effect of the resulting composite PES membranes may be ascribed to the functional groups as well as the hydrophilic characteristics of the inorganic particles [14]. Studies also indicate that inclusion of small amounts of hydrophilic polymeric molecules such as polyethylene glycol (PEG), polyacrylic acid, polyvinylpyrrolidone and polyvinyl alcohol to the casting dope ensures the uniform dispersion of the inorganic modifier throughout the PES membrane matrix as well as increase the modifier's binding strength to the main polymer chain [15–18]. In addition, these polymeric additives greatly regulate the pore formation mechanism, thus impacting the morphology of the resulting blend membranes [19]. Among various polymeric additives mixed with PES membranes, PEG is of special interest. In addition to uniform particle dispersion, PEG increases the cast solution viscosity and thus enhances better pore interconnectivity when added in the optimum amount [19,20]. Also, the polyanionic nature of PEG molecule helps in strong binding of the inorganic additives (especially metals) to PES matrix [21].

Lithium salts have been used as an effective inorganic additive for the polymeric membranes resulting in high flux and enhanced rejection [22–24]. Incorporation of lithium bromide (LiBr) in PES matrix with PEG as pore regulator increased the separation performance of the membrane. Addition of LiBr up to 2 wt% to PES increased the water permeation and protein rejection as compared with lithium chloride and lithium fluoride [22]. Inclusion of LiClO₄ to polyvinylidene fluoride (PVDF) using dimethylacetamide (DMAC) as the solvent produced membranes with uniform pore distribution, resulting in high gas permeation fluxes [23]. Similarly surface modification of PVDF using LiClO₄ as the additive and DMF as the solvent resulted in membranes with increased number of smaller

pores (in several nanometers) ensuring high permeation fluxes and better solute rejections [24].

The main objective of the present study is to modify PES with LiClO₄ to develop novel hydrophilic nanoporous membranes with better anti-fouling properties. A fixed amount of low molecular weight PEG (PEG200) is to be used as the binding agent for the LiClO₄ modifier and also as a pore regulator. The concentration of LiClO₄ was varied in the casting dope to study its effect in the performance of the membranes. Morphology and structural analysis of the pure and blended membranes were examined using scanning electron microscopy and atomic force microscopy techniques. Membrane properties such as equilibrium water content, hydrophilicity and pure water flux were evaluated for the pristine and composite PES membranes. Dye rejection capacity of the neat and blended PES membranes was analyzed using in-house dye solutions. Fouling analysis for all the prepared membranes was done through flux recovery ratio method. The obtained results for the characterization and performance analysis of the composite membranes were compared with the features of the pristine PES membrane.

2. Materials and methods

2.1. Materials

Polyethersulfone (PES, Veradel 3200P) in powder form was supplied by Solvay Specialities India Pvt. Ltd. (India) and it was dried at 120°C for 8 h before being used. Lithium perchlorate (99.99%) was acquired from Sigma-Aldrich Ltd. (India). N,N-dimethylformamide (DMF, 99%) solvent and polyethylene glycol ($M_w = 200$) were obtained from SRL Chemicals Ltd. (India). Dyes such as Congo red ($M_w = 696.7$), Crystal violet ($M_w = 407.9$) and Methylene blue ($M_w = 319.9$) in powder form were obtained from local dyeing industries at Tirupur, Tamil Nadu (India) as gift samples. The molecular structures of all the dyes are presented in Table A1. Freshly prepared deionized water was employed for the preparation of gelation bath, dye solution preparation and membrane storage. All the reagents used in the study were of analytical grade and were applied as such in the experimental methods.

2.2. Membrane preparation

Asymmetric PES ultrafiltration membrane was prepared via wet phase inversion method [25] using casting solution containing PES, PEG200 and LiClO₄ in DMF as solvent. The composition of the various membranes prepared is shown in Table 1. Preparation of the homogenous casting dope was

Table 1
Composition and AFM characterization results of membranes

Membrane ID	Membrane composition (wt %)				Average pore size (nm)	Surface porosity (%)	Roughness (nm)		
	PES	PEG	LiClO ₄	Solvent (DMF)			S_a	S_q	S_z
M0	18	0	0	82	21.8	15.4	19.8	24.6	193
M1	18	2	0	80	17.5	19.5	21.3	26.8	210
M2	18	2	1	79	25.6	24.9	28.3	33.8	329
M3	18	2	3	77	31.5	29.2	31.2	38.2	385
M4	18	2	5	75	85.7	40.8	56.4	65.1	491

done by simultaneous mixing of all components in DMF solvent through mechanical stirring for 8 h at room temperature. The solution was then allowed to stand for 2 h to remove any air bubbles formed during mixing. Subsequently, the solution was casted on a clean glass plate to a thickness of 200 μm using a self-made film applicator. This spread film was immediately admitted to the non-solvent water bath at room temperature without any evaporation, to induce wet phase inversion. After the displacement of the primary solvent and membrane formation, the membranes were moved to fresh water bath for 24 h to ensure complete phase inversion. The prepared membrane sheet was then stored in deionized water till usage.

2.3. Membrane characterization

Morphology of the top surface and the cross section of the prepared membranes was investigated by scanning electron microscopy (SEM) (Evo-18, Carl Zeiss, USA). The membrane sample was cut into small pieces, dried using a filter paper, snapped in liquid nitrogen (for 30 s) and sputtered with gold before obtaining the SEM micrographs.

Surface roughness of the synthesized membranes was measured by atomic force microscopy (AFM) (SPM CP-II, Veeco Co., USA). Samples were cut into rectangular pieces of 10 mm by 10 mm and areas of $1\ \mu\text{m} \times 1\ \mu\text{m}$ of each sample was analyzed by tapping mode. Mean pore size of the membrane surfaces was estimated from the AFM topographic images using SPIP software (version 6.7.3).

Hydrophilicity of the pristine and composite membranes surface was measured in terms of water contact angle. The static contact angle on the membrane surface was obtained using a goniometer (DGX Digidrop, France). The contact angle of each membrane was evaluated by averaging the static contact angles measured at four different positions on the membrane sample's surface.

Equilibrium water content (EWC) of the prepared membranes was calculated by observing the water uptake capacity of the respective membrane sample. Rectangular cut of membrane sample (30 mm by 50 mm) was soaked in deionized water for 24 h. The wet weight of the membrane sample was then measured. Subsequently the wet sample was placed in a vacuum oven at 80°C for 24 h. The dry weight of the membrane sample was then weighed until the weight became constant. EWC of the membrane sample was calculated using Eq. (1), where W_w (kg) and W_d (kg) are the wet and dry membrane weights, respectively, as given below:

$$\text{EWC} = \left(\frac{W_w - W_d}{W_d} \right) \times 100 \quad (1)$$

2.4. Permeation and separation performance

Permeation and separation properties of membranes were examined in a dead-end stirred cell filtration system. The stirred cell (Amicon, Model 8400, Millipore, USA) houses flat sheet membrane pieces with an effective area of 45.6 cm^2 . The feed side of the stirred cell was pressurized using nitrogen gas. The schematic representation of the set-up is shown in

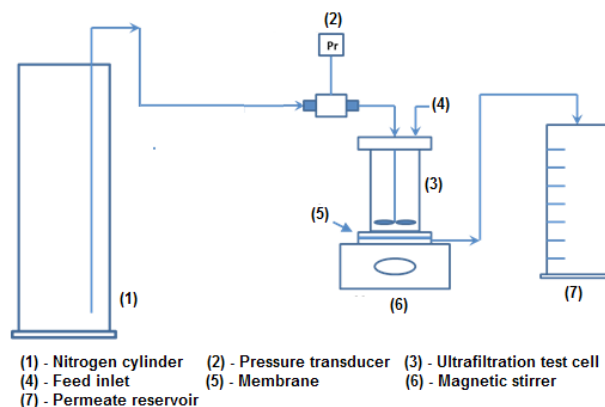


Fig. 1. Schematic representation of the dead-end filtration unit.

Fig. 1. Distilled water and dye solutions were used as feed for evaluation of membrane performance. All membranes were compacted for 2 h at 414 kPa to obtain steady-state flow. Pure water flux (J_w) as well as the dye permeate flux (J_{CR} , J_{CV} , J_{MB}) of all the membranes was measured at a transmembrane pressure of 414 kPa using Eq. (2) as given below:

$$J = \frac{Q}{A \times \Delta t} \quad (2)$$

where J ($\text{L m}^{-2} \text{h}^{-1}$) is the permeate flux, Q (L) is the volume of sample collected; A (m^2) is the effective membrane area and Δt (h) is the sampling time.

Dye rejection efficiencies of the prepared membranes were estimated using Congo red, Crystal violet and Methylene blue solutions as probe molecules. The feed concentration for all dye solutions was taken as 0.1 g L^{-1} . Dye permeate was collected over defined time intervals in graduated tubes and the tube contents were analyzed for dye concentration. Solute rejection percentage (%SR) was calculated using Eq. (3) as follows:

$$\% \text{SR} = \left(1 - \frac{C_p}{C_f} \right) \times 100 \quad (3)$$

where C_p and C_f are the dye concentrations (g L^{-1}) in the permeate and feed streams, respectively. The dye concentration in feed and permeate streams for all the dye solution rejection tests was measured using a Ultraviolet-visible spectrophotometer (UV-3600, Shimadzu Corp., USA) at their respective peak absorption bands as specified in Table A1.

2.5. Fouling analysis

Fouling analysis for the pure and blend membranes was carried out in the same setup used for the water flux and rejection tests. One 'dye-cycle run' for a given membrane consists of 8 h of continuous dye solution filtration, followed with cleaning of the membrane for 30 min in distilled water and 2 h of pure water permeation through it. After five dye-cycle runs, the pure water flux of the fouled membrane (J_{wf}) was

estimated and the flux recovery ratio was calculated using Eq. (4). All experiments were performed at a transmembrane pressure of 414 kPa.

$$\text{Flux recovery ratio} = \left(\frac{J_{wf}}{J_w} \right) \times 100 \quad (4)$$

Membrane fouling can be quantified by the resistance to mass transport across the membrane. For a fouled membrane, the resistance is due to the intrinsic membrane resistance (R_m) as well as the fouling resistance (R_f). In general, the permeate flux (J), through the membrane, may be described by Darcy's law as given in Eq. (5) [26] as follows:

$$J = \frac{\Delta P}{\eta R_t} \quad (5)$$

where ΔP , η and R_t are the transmembrane pressure (Pa), viscosity of the permeate (Pa s) and total resistance for mass transport across the membrane (m^{-1}), respectively. The intrinsic membrane resistance of the membrane (R_m) is commonly obtained from initial pure water flux study (conducted on a fresh membrane) and is calculated using Eq. (6) as given below:

$$R_m = \frac{\Delta P}{\eta J_w} \quad (6)$$

Fouling resistance (R_f) caused by pore plugging and irreversible adsorption of foulants on membrane pore wall is calculated using Eq. (7) as given below:

$$R_f = \left(\frac{\Delta P}{\eta J_{wf}} \right) - R_m \quad (7)$$

Normally, the total resistance (R_t) for mass transport includes the inherent hydraulic resistance of the membrane (R_m) and the resistance due to fouling (R_f).

3. Results and discussions

Addition of PEG to PES polymer chain influences the pore formation during immersion precipitation process owing to strong hydration and large excluded volume in aqueous systems [27]. In order to prevent the strong effect of PEG on pore size, a light molecular weight variant of 200 Da at a low concentration of 2 wt% was included to the casting dope. This 2 wt% of PEG200 was reported to result in desirable and optimum pore sizes by related research works [22,27,28]. Hence in the current study, a 2 wt% of PEG200 was added as fixed amount to the casting dope. The effect of LiClO₄ on various membrane attributes of PES/PEG200 blend is discussed in the below section.

3.1. Scanning electron microscopy studies

SEM images of the top surface and cross sections of pure and blend membranes are shown in Figs. 2 and 3. All membranes

exhibited asymmetric structure and consisted of a skin layer and support layer. Visual comparison of the surface SEM images of the membranes, as shown in Fig. 2 (and Fig. S1), clearly indicated the formation of high nanoporous membrane with large number of surface nanopores due to the addition of PEG200 and LiClO₄. This was due to the enhanced interfacial tension between the two immiscible phases and reduced mass transfer rate of the primary solvent at the surface which was caused by the LiClO₄ addition. However, there was a slight increase in pore size when the concentration of LiClO₄ was increased from 3 wt% to 5 wt%. Enlargement in surface pore size is due to agglomeration effect of the inorganic modifier which was preferentially leached out during the phase inversion resulting in larger pore size. Cross-section SEM images of the membranes, as presented in Fig. 3 (and Fig. S2), exhibit the typical asymmetric structure and the formation of finger-like sub-layer due to LiClO₄ addition. Inclusion of LiClO₄ increased the length of microvoids and made the pore wall wider up to 3 wt%. This can be explained by the hydrophilic nature of the LiClO₄ which caused a faster solvent (DMF) and non-solvent (water) exchange during the phase inversion, resulting in broader finger-like channels with enhanced porosity. Increase of modifier concentration from 3 wt% to 5 wt% resulted in the collapse of the finger-like sub-layer. This was due to the dominant viscous effect (than the hydrophilic effect) of the high concentrations of LiClO₄ in the casting dope. This hindered the polymer demixing rate during membrane formation resulting in spongy support layer. The skin layer thickness of M5 membrane (5 wt% LiClO₄) was also very dense as compared with other membranes. This was again due to the delayed demixing of the solvent and non-solvent resulting in membrane densification.

3.2. Atomic force microscopy studies

Average pore size of prepared membrane surfaces were obtained from AFM images using SPIP software. Surface pore analysis was done using the height profile study of two dimensional AFM image obtained over 1 μm \times 1 μm area of each membrane (as shown in Fig. 4 [and Fig. S3]) and the average values are reported in Table 1. The obtained values clearly indicated that membranes with nano-sized pores were obtained. A small decrease in pore size was observed in M1 membrane due to the pore constriction effect of PEG200. Similar results have been reported by other researchers [22,28]. Increase in pore size from M2 to M4 membranes indicated the pore dilation effect of the LiClO₄ inclusion in the casting dope. Addition of LiClO₄ caused interfacial stresses between polymer and modifier which was released by the formation of larger nanopores due to the shrinkage of organic phase during the demixing process. Also, a drastic increase in the pore size was seen when LiClO₄ concentration was increased from 3 wt% (M3) to 5 wt% (M4). Porosities of the prepared membranes were measured through AFM images using the technique described elsewhere [29]. Increase in surface porosity could be ascribed due to the increase in the number of pores as well as increase in the pore size. The former effect was primarily visualized up to 3 wt% of LiClO₄ while the latter effect was predominant for LiClO₄ concentration above 3 wt%.

Surface roughness parameters of the membranes in terms of the mean roughness (S_u), the root mean square of

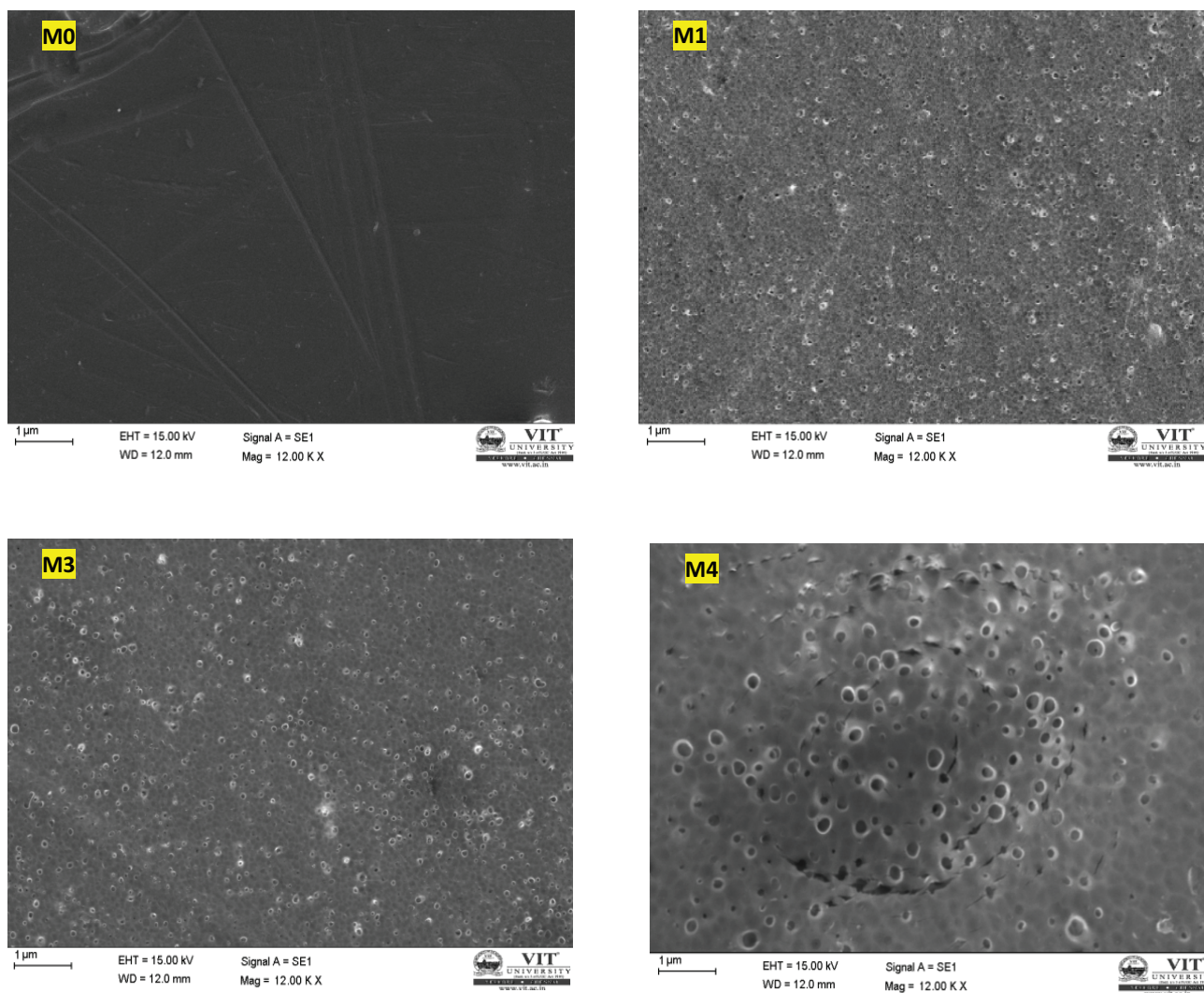


Fig. 2. Surface SEM images of the membranes.

the surface roughness (S_q) and the mean difference between the highest peaks and lowest valleys (S_z) were calculated from AFM images. As shown in Table 1, addition of PEG and LiClO_4 to PES matrix, increased the surface roughness of the resulting membranes. However the magnitude of roughness increase in the blend membrane was very less as compared with surface roughness of pristine PES membrane, indicating the chances of minimal reversible fouling effect in the modified PES membranes.

3.3. Hydrophilicity, equilibrium water content and pure water flux studies

Surface hydrophilicity studies are usually carried out by contact angle measurements [30]. Low contact angle value of a membrane surface indicates the pronounced hydrophilicity in the membrane. As shown in Table 2, contact angles of the membrane surface got decreased with increase in LiClO_4 concentration. Decrease in the contact angle clearly demonstrated that a more hydrophilic surface was obtained due to LiClO_4 addition. Attachment of the polar functional groups

to the active sites of LiClO_4 molecules was seen as a plausible cause for increase in surface wettability. It has been reported that the membrane surfaces with enriched wettability would reduce membrane fouling to a larger extent [31]. Hence the prepared LiClO_4 blend membranes are expected to have better anti-fouling abilities than the pristine PES membrane.

EWC studies showed a considerable rise in water uptake capacity from 38.4% of the pristine PES membrane to a maximum of 59.2% for the LiClO_4 doped PES membrane. This indicated the dominant hydrophilic effect of LiClO_4 which enhanced the porous nature in the composite PES membranes. As evident from SEM images, the large size macrovoids present in the support layer of the lithium blend membranes attributed for the increased water uptake. However the EWC of the PES/PEG/ LiClO_4 blend membranes had a sluggish increase when the LiClO_4 concentration was varied from 3 wt% to 5 wt%. This was mainly because of the collapse of the finger-like sub-layer and the formation of spongy support layer due to the delayed liquid – liquid demixing. In general, the EWC for all LiClO_4 blend membranes was higher than the pristine PES membrane.

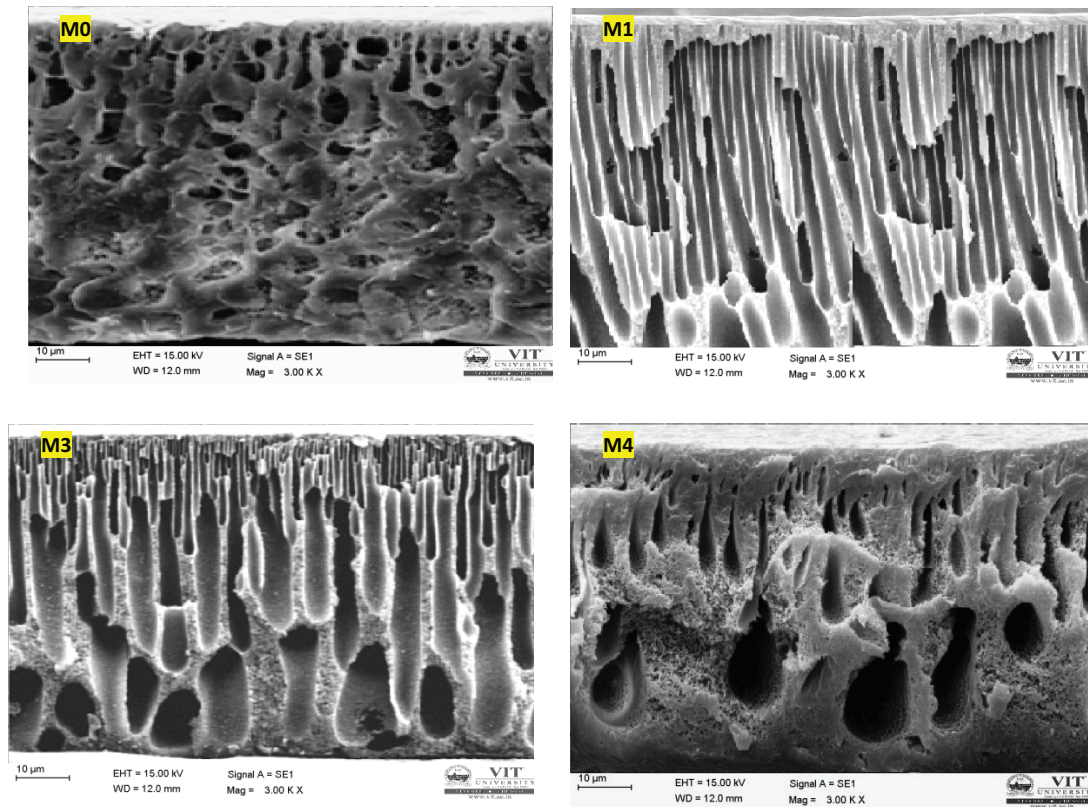


Fig. 3. Cross-section SEM images of the membranes.

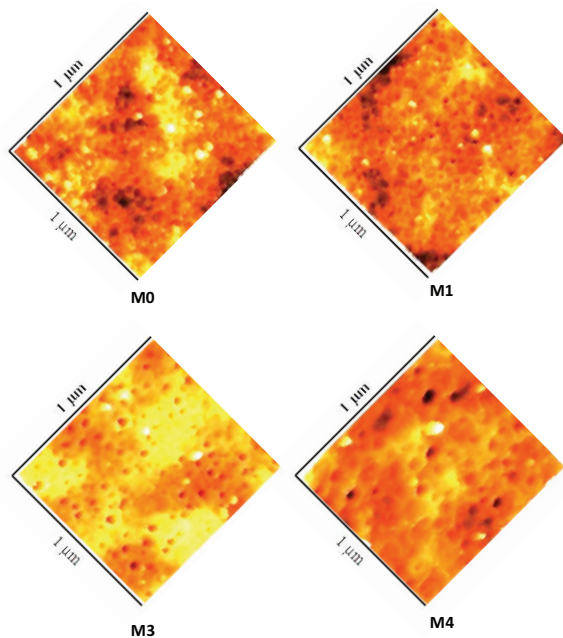


Fig. 4. Surface AFM images of the membranes

The moderate increase in the EWC of the LiClO_4 doped PES membranes was an indication of possible high permeate flux through them without substantial loss on their mechanical strength, as very high water uptake can lead to the loss of mechanical stability.

Pure water fluxes for different prepared membranes are depicted in Fig. 5. All of the modified PES membranes recorded higher water flux as compared with unmodified PES membrane. Maximum pure water flux of $219.3 \text{ L m}^{-2} \text{ h}^{-1}$ was recorded by the M3 (3 wt% LiClO_4) membrane which was nearly five times as high as the water flux of pure PES membrane. Increase in water flux with incremental amounts of LiClO_4 was observed till 3 wt% concentration. This could be explained by the pronounced hydrophilic effect of LiClO_4 which resulted in slightly larger surface pores and well-connected sub-layer. However, when the concentration of LiClO_4 was more than 3 wt%, a decrease in water flux was noted. This was due to the densification of the skin layer and collapse of the finger-like support layer in spite of the hydrophilic effect of the LiClO_4 . Results obtained for pure water flux studies were in good agreement with the inferences made from SEM analysis.

3.4. Dye rejection performance

Rejection characteristics of an asymmetric membrane are controlled by various phenomena associated with active skin layer [2]. Compacted pure and blend membranes were subjected to dye removal studies using Congo red (CR), Crystal violet (CV) and Methylene blue (MB) as test samples. The obtained results are presented in Figs. 6 and 7. As shown in Fig. 6, the dye rejection obtained by M3 membrane with 3 wt% LiClO_4 was highest among the synthesized membrane series. Though the smallest surface pore sizes were observed for M0 and M1 membranes (pure PES and PES/PEG200

Table 2

Contact angle, equilibrium water content and fouling recovery ratio of membranes

Membrane ID	Contact angle (°)	Equilibrium water content (%)	Fouling recovery ratio (%)		
			Congo red	Crystal violet	Methylene blue
M0	55.8	38.4	75.1	79.3	81.4
M1	50.9	47.3	79.3	82.9	84.6
M2	45.8	51.1	88.1	90.5	93.4
M3	39.6	57.5	91.7	93.3	94.7
M4	36.2	59.2	86.5	89.8	93.0

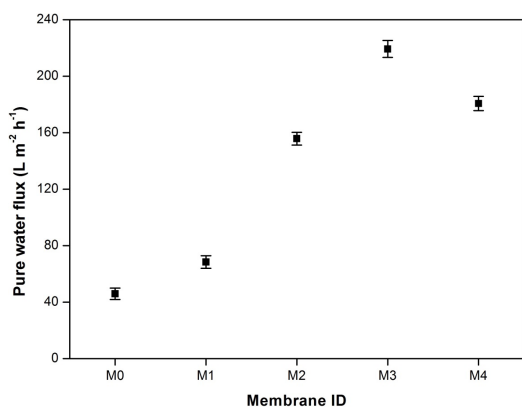
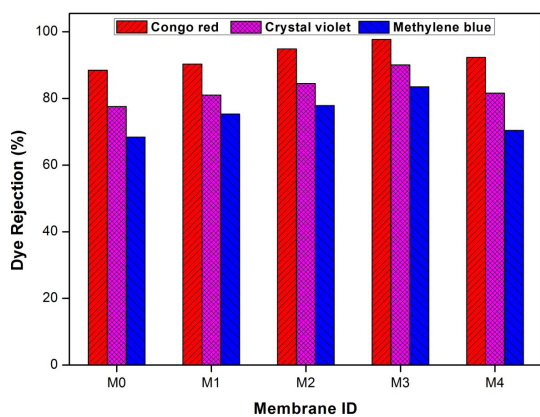
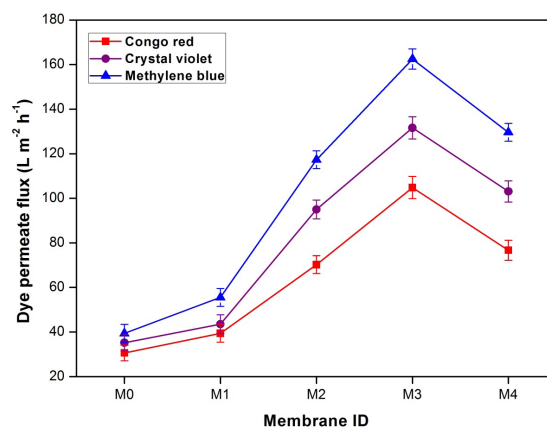


Fig. 5. Pure water flux of unmodified and modified PES membranes.

Fig. 6. Dye rejection efficiencies of PES, PES/PEG and PES/PEG/LiClO₄ membranes.

membrane), the dye rejection ability of all of the LiClO₄ doped membranes were higher. Adsorption of dye molecules on the active sites of LiClO₄ particles present on the surface was a secondary factor, in addition to size exclusion, for the better dye rejection efficiencies of LiClO₄ blend membranes. Similar results for dye adsorption capacity of lithium salts have already been reported [32,33]. Uniform distribution and non-agglomeration of the LiClO₄ particles in M3 membrane contributed for its superior dye separation efficiencies. Dye rejection efficiencies followed the order of CR > CV > MB. Among the various dyes used, CR dye recorded the highest

Fig. 7. Dye permeate fluxes of PES, PES/PEG and PES/PEG/LiClO₄ membranes.

dye rejection of around 90% while the other dyes had a rejection efficiency of less than 90%. This observation could be used to infer that the molecular weight cut-off for the LiClO₄ blend membranes to be 700. Steric hindrance and adsorption were identified as the major separation phenomena for the PES/PEG200/LiClO₄ blend membrane systems.

Steady-state permeate fluxes obtained for the dye rejection studies are presented in Fig. 7. Variation of dye fluxes obtained for the prepared membranes were similar to their respective pure water flux trend. Dye fluxes followed the order of MB > CV > CR for all membranes, which was the reverse of the rejection efficiency pattern. All of the LiClO₄ blend membranes had an improved solute flux than the pristine PES and PES/PEG (0% LiClO₄) membrane. Addition of hydrophilic LiClO₄ produced loose polymer entanglements resulting in higher porosity and thereby high fluxes. Consequently, the solute molecules were able to permeate more easily through the membrane. Also, the hydrophobic tail of the dyes interacted with the membranes while the hydrophilic head was still available which resulted in the high permeate flux for the LiClO₄ blend membranes. Highest dye permeate fluxes was recorded for the M3 membrane for all the dye solutions studied.

3.5. Fouling analysis

Fouling recovery ratio (FRR) of various dyes for all of the prepared membranes were estimated and the results are presented in Table 2. FRR can be viewed as the recycling

ability of a membrane. High value of FRR denotes a better anti-fouling nature of the membrane and hence an extended durability of usage for the membrane. Obtained results clearly indicated that all of the membranes containing LiClO_4 possessed higher FRR as compared with membranes in which LiClO_4 was absent. High FRR values for LiClO_4 doped membranes can be explained through the concept of surface pore size and hydrophilicity of the membranes. Nano-size surface pore sites with size less than molecular diameter of the dye molecules prevented them from entering the membrane and thereby reduced the pore blockage. On the other hand, improved surface hydrophilicity decreased the dye molecule bondage on the surface as well as within the pore wall. Both these effects were comparatively strong for 3 wt% LiClO_4 membrane while for other prepared membranes one of these effects was less pronounced. Thus, M3 membrane had the highest FRR for all the dyes employed in the fouling studies. As seen in Table 2, for any given membrane, the FRR of MB dye was better than the FRR of CV dye and CR dye due to less retention of MB dye by the membrane as compared with CV and CR dye retentions.

Fig. 8 illustrates the intrinsic membrane resistance (R_m) and the fouling resistances due to various dyes ($R_{f,CR}$, $R_{f,CV}$ and $R_{f,MB}$) for each of the prepared membrane. M3 membrane with 3 wt% LiClO_4 possessed the lowest R_m value as well as lowest dye fouling resistances of $R_{f,CR}$, $R_{f,CV}$ and $R_{f,MB}$ among the synthesized membrane series. From the obtained resistance values, it was understood that the intrinsic membrane resistance (R_m) was the controlling factor of mass transport for membranes devoided of LiClO_4 (M0 and M1 membranes), while for LiClO_4 incorporated membranes, both intrinsic membrane resistance as well as the respective dye fouling resistances decided the mass transport of the dye across the membrane. For LiClO_4 doped membranes M2, M3 and M4, the high value of $R_{f,CR}$ as compared with their respective R_m is due to maximum retention of CR dye as compared with M1 and M2 membranes. The retention was induced by the pore size as well the dye adsorption on the added LiClO_4 modifier.

Analyzing the results of the membrane characterizations, dye rejections and fouling studies, it was clear that the 3 wt% LiClO_4 composite membrane possessed better separation and

anti-fouling properties in comparison with the other synthesized membranes.

4. Conclusion

High performance nanoporous PES membranes modified with fixed amount of polyethylene glycol (PEG200) and varying amounts of lithium perchlorate (LiClO_4) were reported for the first time. Prepared membranes were characterized for membrane morphology, surface hydrophilicity, water uptake, porosity, pure water flux, dye rejections and fouling analysis. SEM studies confirmed that inclusion of LiClO_4 resulted in large number of surface pores with well-connected finger-like sub-layer. AFM studies on the prepared membranes confirmed the formation of nano-size surface pores due to LiClO_4 addition to PES. Moderate increase in surface porosity and low increase in surface roughness with incremental amount of LiClO_4 was reported in composite membranes. Contact angle and water uptake measurements proved that the LiClO_4 addition enhanced the hydrophilicity of resulting PES membranes. Performance analysis showed that the pure water flux of the LiClO_4 blend membranes was greatly enhanced to a maximum of five times as compared with pristine PES membrane. Dye rejection studies using several in-house dye solutions clearly exhibited the elevated rejection capacity of the LiClO_4 blend membranes. Steric hindrance and adsorption were identified as the dominant separation mechanisms in the prepared LiClO_4 mixed PES membranes. Fouling analysis indicated the excellent anti-fouling ability of the LiClO_4 doped PES membranes as compared with pure PES membrane. A close analysis on the obtained results revealed the better membrane characteristics of 3 wt% LiClO_4 membrane among the synthesized series of the composite PES membranes. Mass transport modeling along with detailed study of adsorption kinetics for the prepared membranes is a potential scope for future work. Performance of the prepared LiClO_4 incorporated PES membranes towards real-time industrial effluent treatment is to be subsequently carried out as an extension of the current research work. Thus PES/PEG200/ LiClO_4 composite membrane seems to be a promising candidate for treatment of dye polluted wastewater, ensuring high fluxes and improved rejection rates.

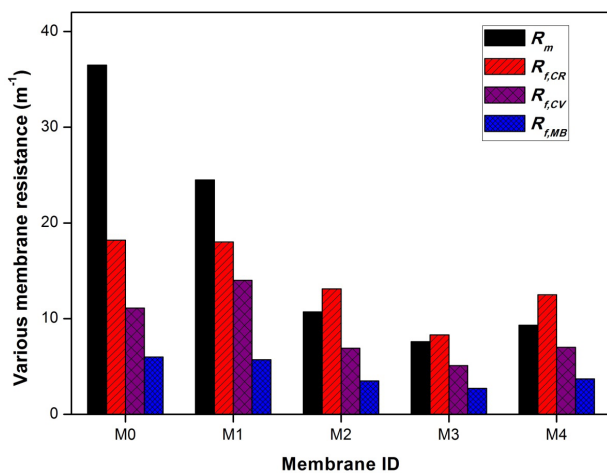


Fig. 8. Filtration resistances of the prepared membranes.

Symbols

M_w	—	Molecular weight
S_d	—	Mean surface roughness
S_d^2	—	Root mean square of surface roughness
S_z	—	Mean difference between the highest peaks and lowest valleys
W_d	—	Weight of dry membrane
W_w	—	Weight of wet membrane
J	—	Permeate flux
J_w	—	Pure water flux (fresh membrane)
J_{CR}	—	Congo red dye permeate flux
J_{CV}	—	Crystal violet dye permeate flux
J_{MB}	—	Methylene blue dye permeate flux
Q	—	Permeate volume through the membrane
A	—	Effective surface area of the membrane
Δt	—	Sampling time
C_p	—	Solute (dye) concentration in the permeate

C_f	—	Solute (dye) concentration in the feed
J_{wt}	—	Pure water flux through the fouled membrane
ΔP	—	Transmembrane pressure
η	—	Dynamic viscosity of permeate
R_t	—	Total resistance for mass transport across the membrane
R_m	—	Intrinsic membrane resistance
R_f	—	Fouling resistance of the membrane
$R_{f,CR}$	—	Congo red dye fouling resistance of the membrane
$R_{f,CV}$	—	Crystal violet dye fouling resistance of the membrane
$R_{f,MB}$	—	Methylene blue dye fouling resistance of the membrane
wt%	—	Weight percentage

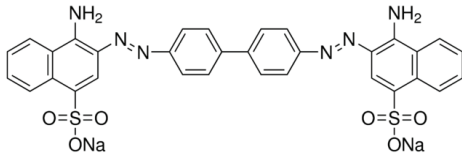
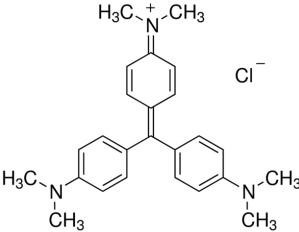
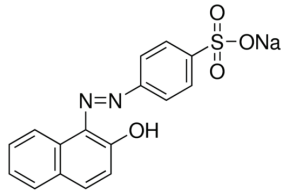
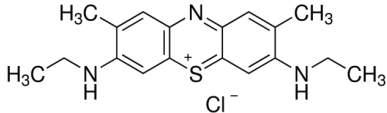
References

- T.H. Kim, C. Park, S. Kim, Water recycling from desalination and purification process of reactive dye manufacturing industry by combined membrane filtration, *J. Cleaner Prod.*, 13 (2005) 779–786.
- W.J. Lau, A.F. Ismail, Polymeric nanofiltration membranes for textile dye wastewater treatment: preparation, performance evaluation, transport modeling, and fouling control—a review, *Desalination*, 245 (2009) 321–348.
- M. Mulder, *Basic Principles of Membrane Technology*, Kluwer Academic Publishers, London, 1996.
- A.L. Ahmad, A.A. Abdulkarim, B.S. Ooi, S. Ismail, Recent development in additives modifications of polyethersulfone membrane for flux enhancement, *Chem. Eng. J.*, 223 (2013) 246–267.
- M.N. Abu Seman, D. Johnson, S. Al-Malek, N. Hilal, Surface modification of nanofiltration membrane for reduction of membrane fouling, *Desal. Wat. Treat.*, 10 (2009) 298–305.
- K. Rambabu, S. Velu, Modified polyethersulfone ultrafiltration membrane for the treatment of tannery wastewater, *Int. J. Environ. Stud.*, 73 (2016) 819–826.
- H. Yu, Y. Zhang, J. Zhang, H. Zhang, J. Liu, Preparation and antibacterial property of SiO₂-Ag/PES hybrid ultrafiltration membranes, *Desal. Wat. Treat.*, 51 (2013) 3584–3590.
- C.S. Ong, W.J. Lau, P.S. Goh, B.C. Ng, A.F. Ismail, Preparation and characterization of PVDF-PVP-TiO₂ composite hollow fiber membranes for oily wastewater treatment using submerged membrane system, *Desal. Wat. Treat.*, 53 (2015) 1213–1223.
- V.D.N. Medeiros, T.C. de Carvalho, A.M. Leite, E.M. Araújo, H.L. Lira, Evaluation of the effect of clay in polyethersulfone membranes, *Desal. Wat. Treat.*, 56 (2015) 3554–3560.
- H. Basri, A.F. Ismail, M. Aziz, K. Nagai, T. Matsuura, M.S. Abdullah, B.C. Ng, Silver-filled polyethersulfone membranes for antibacterial applications—effect of PVP and TAP addition on silver dispersion, *Desalination*, 261 (2010) 264–271.
- N. Maximous, G. Nakhla, W. Wan, K. Wong, Performance of a novel ZrO₂/PES membrane for wastewater filtration, *J. Membr. Sci.*, 352 (2010) 222–230.
- S. Balta, A. Sotto, P. Luis, L. Benea, B. Van der Bruggen, J. Kim, A new outlook on membrane enhancement with nanoparticles: the alternative of ZnO, *J. Membr. Sci.*, 389 (2012) 155–161.
- Y. Liu, G.H. Koops, H. Strathmann, Characterization of morphology controlled polyethersulfone hollow fiber membranes by the addition of polyethylene glycol to the dope and bore liquid solution, *J. Membr. Sci.*, 223 (2003) 187–199.
- V. Vatanpour, S.S. Madaeni, A.R. Khataee, E. Salehi, S. Zinadini, H.A. Monfared, TiO₂ embedded mixed matrix PES nanocomposite membranes: influence of different sizes and types of nanoparticles on antifouling and performance, *Desalination*, 292 (2012) 19–29.
- R. Krishnamoorthy, V. Sagadevan, Polyethylene glycol and iron oxide nanoparticles blended polyethersulfone ultrafiltration membrane for enhanced performance in dye removal studies, *e-Polymers*, 15 (2015) 151–159.
- A. Rahimpour, S.S. Madaeni, Improvement of performance and surface properties of nano-porous polyethersulfone (PES) membrane using hydrophilic monomers as additives in the casting solution, *J. Membr. Sci.*, 360 (2010) 371–379.
- N. Ghaemi, S.S. Madaeni, P. Daraei, H. Rajabi, S. Zinadini, A. Alizadeh, S. Ghousivand, Polyethersulfone membrane enhanced with iron oxide nanoparticles for copper removal from water: application of new functionalized Fe₃O₄ nanoparticles, *Chem. Eng. J.*, 263 (2015) 101–112.
- S. Pourjafar, A. Rahimpour, M. Jahanshahi, Synthesis and characterization of PVA/PES thin film composite nanofiltration membrane modified with TiO₂ nanoparticles for better performance and surface properties, *J. Ind. Eng. Chem.*, 18 (2012) 1398–1405.
- M.L. Méndez, A.I. Romero, V.B. Rajal, E.F. Castro, J.I. Calvo, L. Palacio, A. Hernández, Properties of polyethersulfone ultrafiltration membranes modified with polyethylene glycols, *Polym. Eng. Sci.*, 54 (2014) 1211–1221.
- A. Idris, N. Mat Zain, M.Y. Noordin, Synthesis, characterization and performance of asymmetric polyethersulfone (PES) ultrafiltration membranes with polyethylene glycol of different molecular weights as additives, *Desalination*, 207 (2007) 324–339.
- Y. Mansourpanah, S.S. Madaeni, A. Rahimpour, A. Farhadian, A.H. Taheri, Formation of appropriate sites on nanofiltration membrane surface for binding TiO₂ photo-catalyst: performance, characterization and fouling-resistant capability, *J. Membr. Sci.*, 330 (2009) 297–306.
- A. Idris, I. Ahmed, M.A. Limin, Influence of lithium chloride, lithium bromide and lithium fluoride additives on performance of polyethersulfone membranes and its application in the treatment of palm oil mill effluent, *Desalination*, 250 (2010) 805–809.
- M.L. Yeow, Y. Liu, K. Li, Preparation of porous PVDF hollow fibre membrane via a phase inversion method using lithium perchlorate (LiClO₄) as an additive, *J. Membr. Sci.*, 258 (2005) 16–22.
- D.J. Lin, C.L. Chang, F.M. Huang, L.P. Cheng, Effect of salt additive on the formation of microporous poly(vinylidene fluoride) membranes by phase inversion from LiClO₄/water/DMF/PVDF system, *Polymer*, 44 (2003) 413–422.
- Y. Lukka Thuyavan, N. Anantharaman, G. Arthanareeswaran, A.F. Ismail, Modification of polyethersulfone using sericin and polyvinylpyrrolidone for cadmium ion removal by polyelectrolyte-enhanced ultrafiltration, *Desal. Wat. Treat.*, 56 (2015) 366–378.
- A.L. Ahmad, A.A. Abdulkarim, S. Ismail, B.S. Ooi, Preparation and characterisation of PES-ZnO mixed matrix membranes for humic acid removal, *Desal. Wat. Treat.*, 54 (2015) 3257–3268.
- A. Rahimpour, S.S. Madaeni, M. Jahanshahi, Y. Mansourpanah, N. Mortazavian, Development of high performance nanoporous polyethersulfone ultrafiltration membranes with hydrophilic surface and superior antifouling properties, *Appl. Surf. Sci.*, 255 (2009) 9166–9173.
- S.R. Panda, S. De, Preparation, characterization and performance of ZnCl₂ incorporated polysulfone (PSF)/polyethylene glycol (PEG) blend low pressure nanofiltration membranes, *Desalination*, 347 (2014) 52–65.
- A. Rahimpour, S.S. Madaeni, Polyethersulfone (PES)/cellulose acetate phthalate (CAP) blend ultrafiltration membranes: preparation, morphology, performance and antifouling properties, *J. Membr. Sci.*, 305 (2007) 299–312.
- H.R. Ahn, T.M. Tak, Y.N. Kwon, Preparation and applications of poly vinyl alcohol (PVA) modified cellulose acetate (CA) membranes for forward osmosis (FO) processes, *Desal. Wat. Treat.*, 53 (2015) 1–7.
- H. Basri, A.F. Ismail, M. Aziz, Polyethersulfone (PES)–silver composite UF membrane: effect of silver loading and PVP molecular weight on membrane morphology and antibacterial activity, *Desalination*, 273 (2011) 72–80.

- [32] S. Natarajan, H.C. Bajaj, Recovered materials from spent lithium-ion batteries (LIBs) as adsorbents for dye removal: equilibrium, kinetics and mechanism, *J. Environ. Chem. Eng.*, 4 (2016) 4631–4643.
- [33] J. Guo, J. Zhang, C. Chen, Y. Lan, Rapid photodegradation of methyl orange by oxalic acid assisted with cathode material of lithium ion batteries LiFePO_4 , *J. Taiwan Inst. Chem. Eng.*, 62 (2016) 187–191.

Appendix

Table A1
Chemical structure and maximum absorption wavelength of dyes

Dye	Maximum absorption wavelength (nm)	Chemical structure
Congo red	495	
Crystal violet	590	
Orange II	486	
Methylene blue	665	

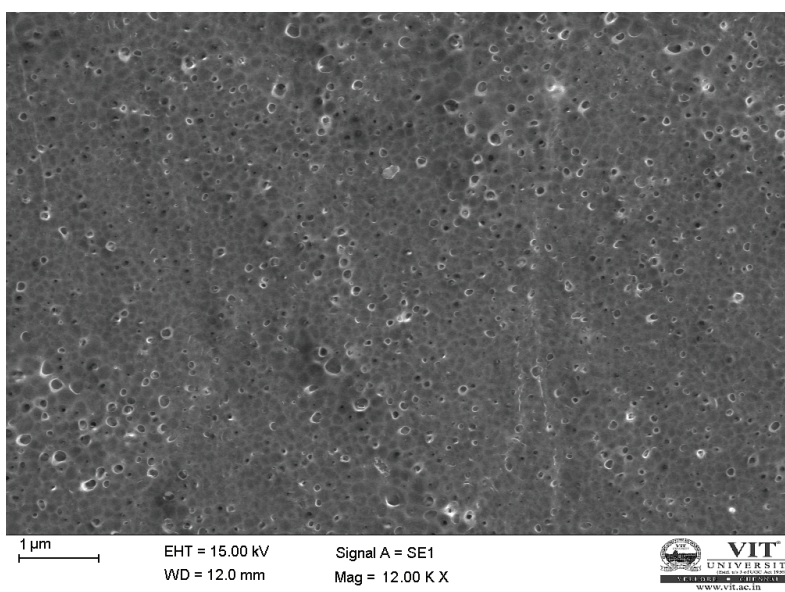


Fig. S1. Surface SEM image of M2 membrane.

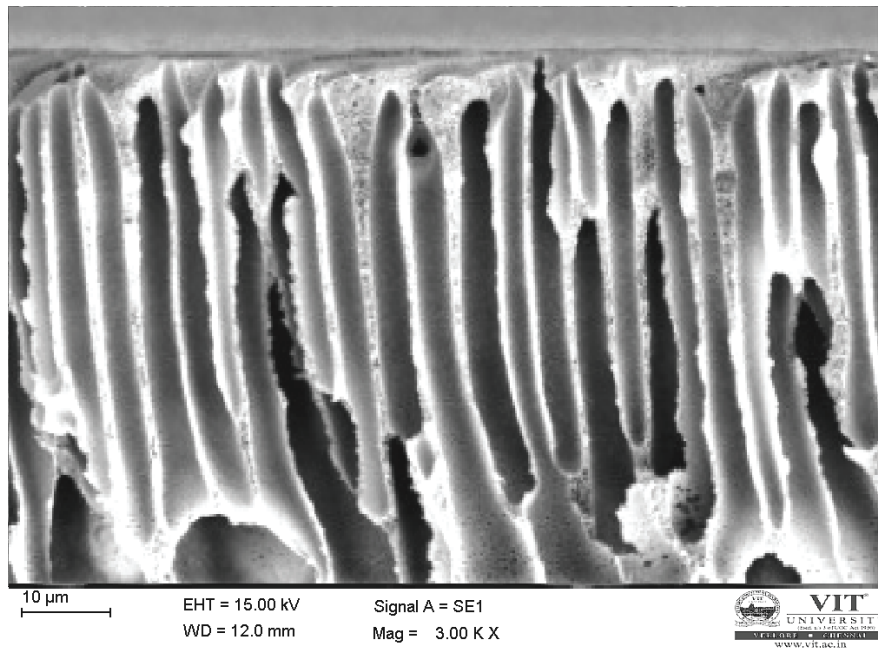


Fig. S2. Cross-section SEM image of M2 membrane.

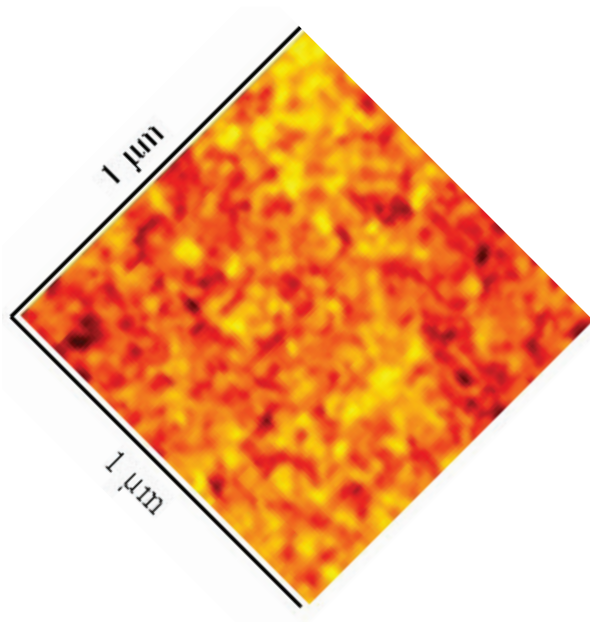


Fig. S3. Surface AFM image of M2 membrane.